



Effect of Soil Improvement on Seismic Behaviors of Anchored Sheet Pile Walls Embedded in Liquefiable Sites

A. Zekri¹, M.H. Aminfar², A. Ghalandarzadeh³, N. Taghizadieh⁴

1-Ph.D student, Faculty of Civil Engineering, University of Tabriz

2, 4- Associated Professor, Faculty of Civil Engineering, University of Tabriz

3- Associated Professor, School of Civil Engineering, Tehran University

ashrafzekri@gmail.com

Abstract

Dynamic response of anchored sheet pile quay walls embedded in liquefaction susceptible soil was investigated numerically utilizing strain space plasticity model for cyclic mobility available in DIANA finite element program. Based on the results, the extension of liquefiable soil around the wall root, leads to the "failure at embedment" mode. Remediation method by deep vibro-compaction of weak area is considered as the liquefaction countermeasure. Effectiveness of soil improvement in zones adjacent to embedded section is discussed based on analytical dynamic responses. Implemented countermeasures are found to considerably reduce deformations of the wall. The compacting of this section not only reduces driving moment applied to the wall root, but also creates resistant moment against root escaping. In addition to the impacts of base acceleration amplitude, the optimum extension of improved zones is introduced.

Keywords: Liquefaction, Sheet pile, Compaction, Numerical.

1. INTRODUCTION

This paper presents the effects of liquefiable layer located adjacent to the embedded section of sheet pile walls investigated physically and numerically. The features of an existing quay wall of Rajaii port, south of Iran were considered as a prototype structure. This reinforced concrete wall is a sheet pile one of totally 35m height. The wall was anchored to concrete piles of about 13m height by cables. Recently exploration showed that along some considerable length, the wall has been embedded in a loose silty sand layer, which is susceptible to liquefaction.

The main objective of this study is to identify the failure mechanism of similar walls and to propose appropriate improvement zone. To this goal, the failure mechanism was recognized and then additional discussion was presented according to numerical modeling results. General results of the numerical modeling were compared with the observations of experimental references. The numerical modeling was conducted using DIANA finite element software [1]. Details of study are presented in following parts.

2. NUMERICAL MODELING

Numerical study was carried out using DIANA finite element software and Towhata-Iai constitutive model. This model is a generalized plasticity-multiple mechanism type. The main feature of this approach is that the concept of the multiple mechanisms, within the framework of plasticity theory defined in strain space, is used as a tool for decomposing the complex mechanism in to set of one dimensional mechanism. The undrained stress path is idealized with the concept of liquefaction front, which is defined in the effective stress space as an envelope of stress points gradually approaching failure line. The liquefaction front is a bilinear function in normalized state parameter and normalized shear stress ratio space [2]. In order to introduce suitable parameters for numerical analysis, the cyclic behavior of Firuzkooh sand no. 161 in cyclic shear test [3] was simulated using the mentioned model and summarized in Table 1. Regarding to construction stages of anchored sheet pile walls and in order to simulate initial stresses, the "phased analysis" method was adapted. During the first phase, a level ground model subjected to self-weight loading was analyzed to obtain vertical and horizontal stresses using K_0 condition. Then the sheet pile wall and the anchor

were embedded in the soil as infinite shell elements. After equilibrium under gravity loading, the soil in front of the wall was removed to the level of the tie rod in -2m. After applying pretension loading, the remained soil elements in front of the wall was removed to level -22m. For all these stages Mohr-Columb criterion and drained condition were used. The stresses obtained in the end of static phase were used as initial stresses in the following dynamic analysis. During dynamic phase, the constitutive model of Towhata- Iai and undrained situation were activated. As base acceleration, a harmonic time history of accelerations with $a_{max} = 0.25g$, and 0.50g in amplitude and 1,2 & 3Hz in frequency were applied to the models for duration of 10sec.

The soil mass was modeled using QU8EPS elements, which are four-node quadrilateral isoparametric plane strain elements. Diaphragm wall and anchor were modeled by infinite shell, CL9PE elements, while the tie rod was modeled by a node-to-node spring, SP2TR element, [1]. According to Kramer (1996) [4] the maximum spatial element size was selected based on the wavelength associated with the frequency through the loose sand. In order to consider wave reflection at the interface of the soil and the bedrock of site, the bottom of the models were modeled as fixed translation boundaries in horizontal and vertical directions, however lateral sides were defined as viscous boundaries. The geometry of the numerical model was shown in Figure 1.

Table1. Material parameters for clean sandy soil layers.

Statue	ρ^{sat} ($\frac{kg}{m^3}$)	K_{ma} MPa	G_{ma} MPa	φ_f (°)	φ_p (°)	W1	P1	P2	C1	S1	Hv
Dr=35%	1900	223	85.85	34	28	4	0.3	3.8	1.5	0.005	0.24
Dr=75%	1980	300	115	40	28	40	0.1	1	1	0.005	0.24
Dr=98%	2000	324	124.5	42	28	42	0.1	0.8	1	0.005	0.24

ρ^{sat} : saturated unit mass; K_{ref} : reference bulk modulus; G_{ref} : reference shear modulus; K_{ref} and G_{ref} are given for ($\sigma'_{m0} = 100kPa$), φ_f : friction angle, φ_p : angle of phase transformation line; P1, P2, W1, S1 and C1: model parameter, Hv: damping factor.

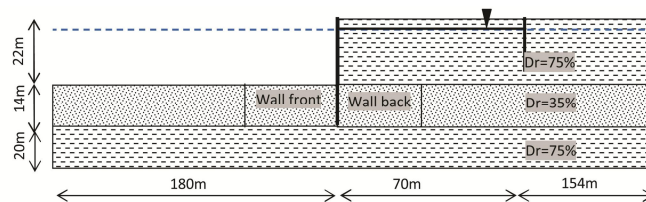


Figure 1. Geometry of the numerical model.

3. ANALYTICAL RESULTS

The mentioned finite element model was also exhibited considerable amounts of deformations. However the magnitudes of displacements are strongly dependent on the characteristics of base acceleration, such as frequency and amplitude. Regardless of the scales of displacements, the final shape of the retaining structure was similar to Figure 2.

Obviously due to base shaking, embedded in liquefiable sand, the bottom of the wall experienced higher displacement rather than its top. This mode of failure was introduced as "failure at embedment". In view of the extension of affected zones, that involved entire elements of retaining system, retrieving the serviceability of structure after this type of failure may be quite costly or even impossible. As marked on Figure 2(b), the deformed mesh indicated that the most visible deformations were localized in loose soil around the embedded section. Beside the noticeable heave of the seabed, its seaward displacement caused significant reduction in its supporting role for the embedded section and led to the large tilt of the wall. Consequently, an active wedge, extended from the embedded section to the back of the anchors, was formed. Moving along this wedge, the anchors endured significant overturning. It is noteworthy that deformed section

of the seabed, in front of the embedded section, was compressed horizontally and extended vertically; whereas the affected section of loose layer, behind the embedded section, was extended horizontally and compressed vertically. Thus the deformation modes were combinations of plane strain and shearing with different directions in both sides of the wall root. However, owing to the relatively low weight of the wall and negligible settlement, the soil beneath the embedded section did not deform visibly. The settlement of dense backfill increased towards the wall while decreased in depth. Observed settlement may be due to: (i) compaction settlement, (ii) settlement caused by lateral spread of active wedge, (iii) both (i) and (ii).

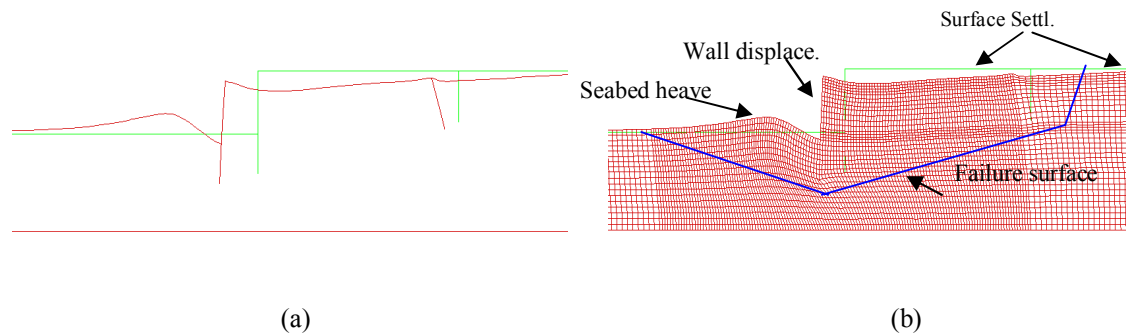


Figure 2. Final shape of the unimproved model, (a) external boundaries, (b) deformed mesh.

The deformation process and final shape of the system demonstrated considerable similarity with physical modeling using shaking table [5]. Figure 3(a) and (b) illustrate initial and final shapes of the model SPM1, respectively. In this model the sheet pile was embedded in liquefiable sand while the backfill and foundation layer constructed by dense sand.

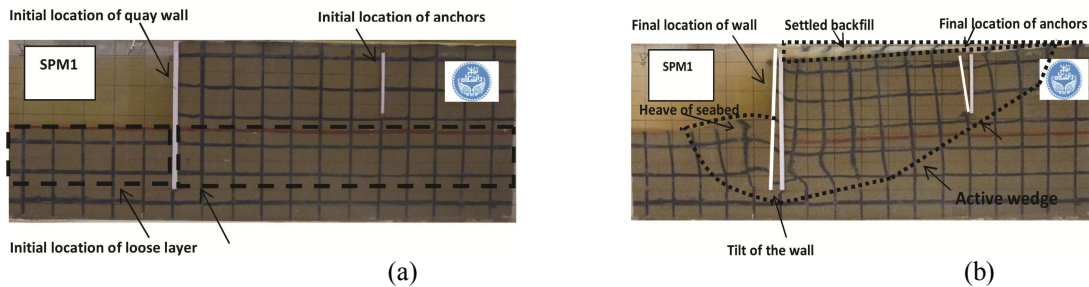


Figure 3. (a) Initial and (b) final shapes of SPM1[5].

As presented in Figure 4(a), the rates of displacements of the wall bottom were higher than those of the wall top, during studied motions. This trend caused the bottom of the wall exceeded the top after some seconds and occurrence of "failure at embedment" mode. Beside this fact that the mode changing happened rapidly in low frequencies, the amount of displacements increased with decreasing in frequency. Comparing the scale of displacements in Figure 4(a) and (b), the growth of displacements due to higher amplitude of base acceleration was obvious.

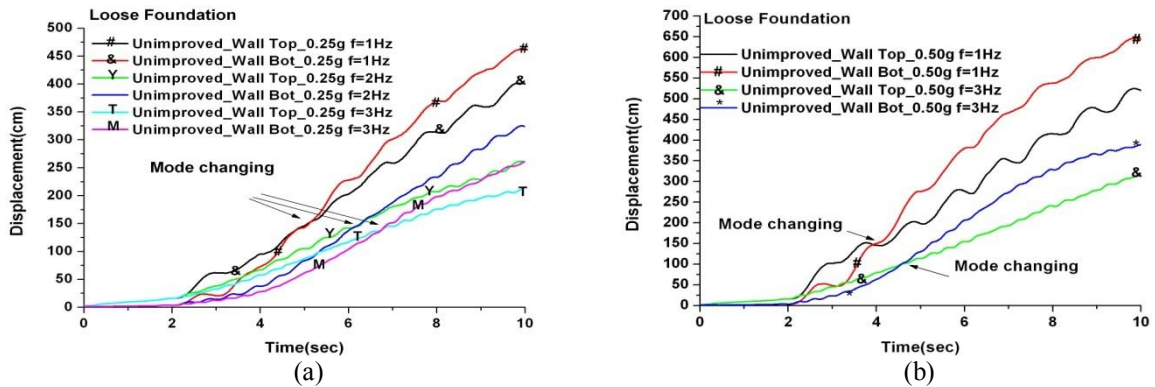


Figure 4. Time history of the top and bottom of the wall, (a) $a_{max}=0.25g$, $f=1, 2 \& 3$ Hz, (b) $a_{max}=0.50g$, $f=1, 3$ Hz.

In order to recognize liquefaction situation, the monotonic component of the excess pore pressure ratio, r_u , was utilized. For instance the liquefaction situations of representative elements are compared in Figure 5 during base acceleration of $a_{max}=0.25g$ and $f=1Hz$. The elements were chosen from the deep level of the loose layer which had higher initial vertical effective stress. From this point of view, and for all studied motions, the monotonic component of excess pore pressure time histories revealed that the seaward zone of the loose layer was the most vulnerable section to develop considerable ratio of excess pore pressure. In addition to the lower initial vertical stress magnitude in this zone, the static shear stress of elements near the excavated side increased liquefaction susceptibility of the zone [4]. In addition, considering the wall tilt direction during base shaking; this zone was subjected to additional decrease in volume that led to more building up in pore pressure, in turn.

In spite of the seaward section of the loose layer, the elements of loose layer located behind the wall root did not experienced significant amounts of r_u . This behavior may be attributed to the higher initial effective vertical stress and to the seaward movement of the wall root that prevented excess pore pressure development in these areas.

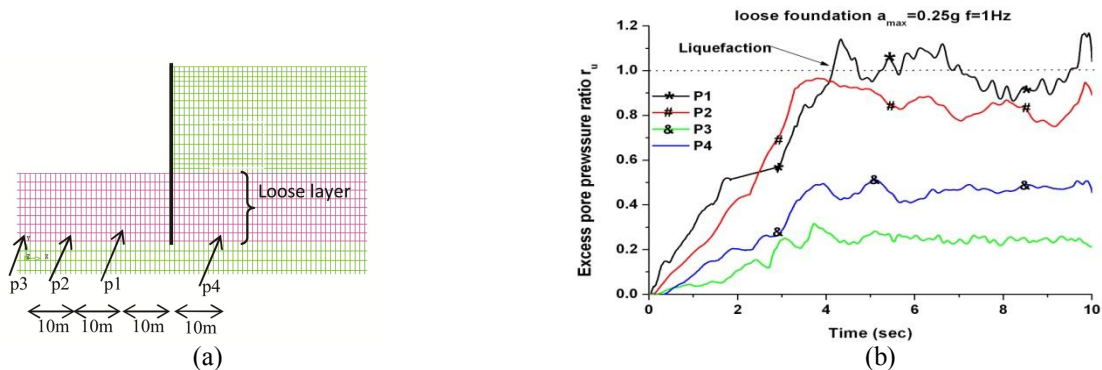


Figure 5. (a) Location of representative elements, (b) time history of excess pore pressure, $a_{max}=0.25g$, $f=1$ Hz.

Regarding to the design methods of sheet piles for static loading, based on "free end" or "fixed earth" assumptions, the trend of bending moment along the wall was studied. Figure 6(a) demonstrates the variation of bending moment along the wall during base acceleration of $a_{max}=0.25g$, $f=1$ Hz. It is obvious that the embedment zone provided significant resistant moment at the beginning of the motion, $t=0.01$ sec. However this moment did not last even by $t=3$ sec. In addition, at $t=5$ sec. considerable overturning moment was applied to the wall root and wall center by the earth pressure. The time history of the average bending moment applied to the middle and bottom elements of the wall, Figure 6(b), proved that the loose layer around the wall root did not provide sufficient resistant moment against overturning moment during dynamic loading. This issue was recognized as the main reason of the "escape" of the wall bottom during base acceleration. To support this idea the time history of average bending moments of the middle and bottom elements of the wall in 2.5Front-2.5Back model, subjected to $a_{max}=0.50g$, $f=1$ Hz was examined. In this model both zones, adjacent to the root front and to root back, were compacted to $Dr=98\%$ along 2.5 times of the root height ($2.5 \times 14m$). As presented in Figure 7(a) the compaction of the loose layer adjacent to the wall

root not only decreased average moment of the central part of the wall, but also prevented existing of the overturning moment at the wall bottom. According to Figure 7(b), the extension of improved zone by 5 times of the root height led to significant reduction in normalized displacements of the wall top and its bottom. However the efficiency of the countermeasure was more pronounced in controlling of the displacements of the wall bottom rather than those of the wall top.

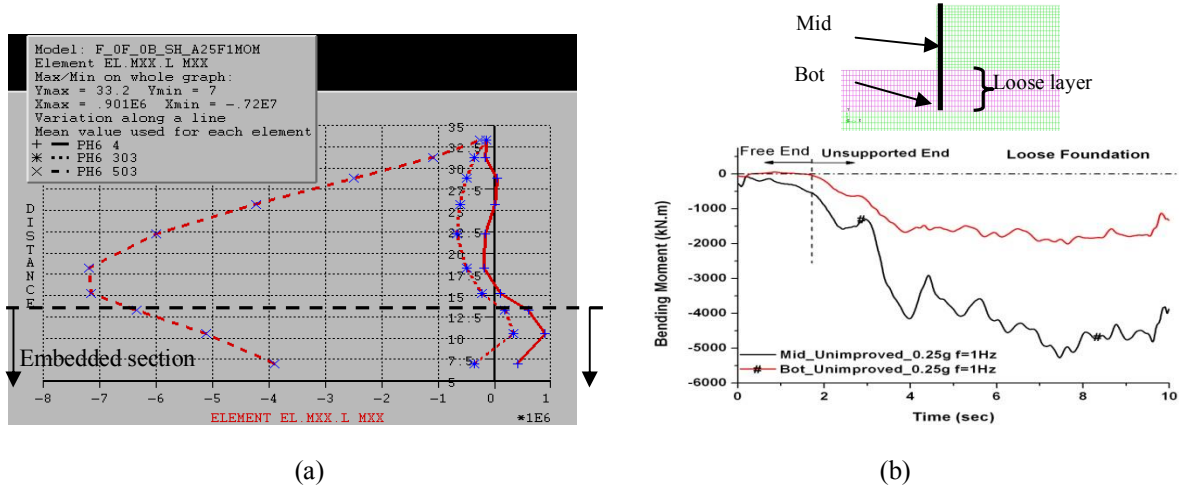


Figure 6. (a) Variation of bending moment along the wall, $t=0.01s$ (PH6 4), $t=3s$ (PH6 303) and $t=5s$ (PH6 503), (b) time history of average bending moment of the middle and bottom of the wall, $a_{max}=0.25g$, $f=1$ Hz.

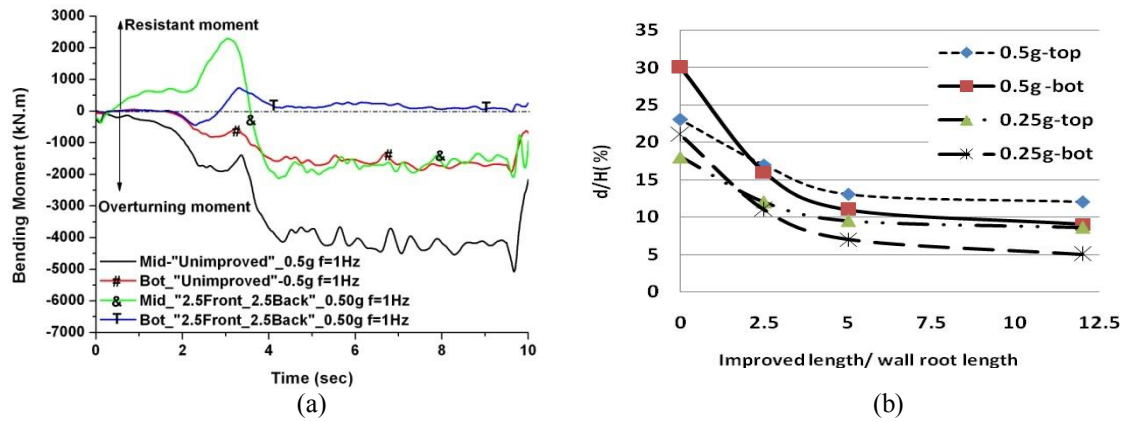


Figure 7. Time history of average bending moment of the middle and bottom of the wall, $a_{max}=0.5g$, $f=1$ Hz.

4. CONCLUSIONS

Based on the model observations and numerical results, the extension of liquefiable layer around the embedded section of the sheet pile caused failure at embedment, in which the bottom of the wall endures higher displacement than the top. Besides the softening of loose layer in front of the wall root due to liquefaction, overturning moment applied to the wall bottom were identified as the main reasons of embedment failure. Compaction of vulnerable zones along both sides of the wall root reduced displacements of the wall top and wall bottom. The efficiency of the mitigation plan was more significant in stabilizing wall bottom.



5. REFERENCES

1. Manie, J. and Kikstra, W.P., (2009)," DIANA User's Manual: Matlib, 1st Edn", TNO DIANA BV, Netherlands.
2. Iai S., Matsunaga, Y., Kameoka, T. (1990), "Strain Space Plasticity Model for Cyclic Mobility", The Port & Harbour Research Institute of JAPAN, Vol. 29, No. 4.
3. Ahmadi, M. and Shirasb, A. (2011), "Liquefaction resistance of Firoozkuh sand using cyclic simple shear test", 6th N. Confr. on Civil Eng., Semnan, Iran (In Persian).
4. Kramer, S.L. (1996). Geotechnical Earthquake Engineering, Prentice Hall.
5. Zekri, A., Ghalandarzadeh, A., Ghasemi, P., Aminfar, M.H," Experimental study of remediation measures of anchored sheet pile quay walls using soil compaction", Ocean Engineering93(2015).45–63